In-Situ Synthesis of Polymer–Clay Nanocomposites: Exfoliation of Organophilic Montmorillonite Nanolayers in Poly 2-Thiozyl Methacrylamide

C. Soykan* and M. Akbay

Department of Materials Science and Nanotechnology, Faculty of Engineering, University of Uşak, 64200-Uşak, Turkey

Abstract: The aim of this work is the preparation and properties of poly 2-thiozyl methacrylamide-vinylbenzyldimethyloctadecylammonium/montmorillonite (TMAAm-VBOA/MMT) nanocomposites. Firstly 2-thiozyl methacrylamide (TMAAm) monomer was synthesized by reacting 2-amino thiazole with methacryloyl chloride in the presence of triethylamine. Synthesis of nanocomposites were performed in three steps which are; purification and cation exchange capacity (CEC) determination of clay, preparation of organoclay and synthesis of nanocomposites. Nanocomposites with various amounts of TMAAm and VBOA/MMT were synthesized through *in-situ* and free radical polymerization using benzoyl peroxide as an initiator. Changes in the structure of the nanocomposites were examined through Fourier transform infrared spectroscopy (FT-IR), X-ray diffractometry (XRD) and scanning electron microscopy (SEM). Additionally, thermogravimetric analysis and BET analysis were conducted to investigate the thermal properties and particle size distribution of the nanocomposites. The results of X-ray and SEM analysis suggest that the exfoliated structure of the new nanocomposite materials. In addition, the thermal decomposition temperatures of nanocomposites were found to be higher than that of pure organoclay and poly(TMAAm) and thermally degradation rate decreased.

Keywords: Montmorillonite, Organoclay, *In-Situ* Polymerization, Nanocomposite, Thermogravimetry.

1. INTRODUCTION

In recent years, interest in polymer-layered silicate (PLS) composites or nanocomposites have rapidly been increasing at an unprecedented level, both in academia and in industry, due to their potential for enhanced chemical, physical, and mechanical properties compared to conventionally filled composites [1-19]. They have the potential of being a low-cost alternative to high-performance composites for commercial applications in both the packaging and automotive industries. The earliest motivation for the use of nanoparticles seems to have been stimulated by the Toyota research group, where the first practical application of nylon-6–montmorillonite (MMT) nanocomposite was commercialized. With only a small MMT loading (4.2 wt%), the heat distortion temperature increased by 100 ^{o}C, the tensile strength increased more than 50%, combustion heat release rate decreased by up to 63% and the modulus doubled [20]. However, in general, all the promises and claims that the addition of nanoparticles to polymer matrices will miraculously lead to exceptional mechanical properties have not been completely fulfilled because the improvements in properties seem to plateau at levels of about 4 wt%. Polymer nanocomposites are two-phase materials in which the polymers are reinforced by nanoscale fillers. The most heavily used filler material is based on the smectite class of aluminum silicate clays, of which the most common representative is montmorillonite (MMT). Montmorillonite is during the past 1/2 decades most preferred commercial layered silicates as nanofiller in the preparation of nanocomposites. However, the hydrophilic nature of montmorillonite limits its compatibility with organophilic polymers. Thus, clay has been rendered hydrophobic to make montmorillonite compatible with organophilic polymer. Due to the presence of exchangeable metal cation such as Li^{+}, Na^{+}, Ca^{2+}, the modification of montmorillonite can be easily achieved with alkyl ammonium salts to form organo-montmorillonite [21-24]. The dispersion of clay into polymer matrix at nanometer-scale leads to significant improvements in the adsorptive, thermal, and mechanical properties of composites. MMT has been employed in many PLS nanocomposite systems because it has a potentially high-surface area and high-aspect ratio that could lead to materials which could possibly exhibit great property enhancements. In addition, it is naturally occurring, readily available in large quantities and environmentally friendly. Most of the engineering polymers are hydrophobic. Layered silicates in their pristine state are hydrophilic. Therefore, dispersion of native clays in most polymers is not easily achieved due to the hydrophobic engineering polymers and the intrinsic incompatibility of hydrophilic-layered silicates [25]. In order to have a successful development of clay-based nanocomposites, it is necessary to chemically modify a

Address correspondence to this article at the Department of Materials Science and Nanotechnology Engineering, Faculty of Engineering, University of Uşak, 64200, Uşak, Turkey; Tel: 0 276 221 21 21; Fax: 0 276 221 21 22;
E-mail: cengizsoykan@usak.edu.tr

E-ISSN: 2410-4701/19

natural clay so that it can be compatible with a chosen polymer matrix. Generally, this can be done through ion-exchange reactions that replace interlayer cations with quarternary alkylphosphonium or alkylammonium cations [26−28]. It is well established that when layered silicates are uniformly dispersed (exfoliated) in a polymer matrix, the composite properties can be improved to a dramatic extent. These improvements may include higher modulus [29,30], barrier properties [31], increased strength [32], thermal stability [33,34] and decreased flammability [33,35]. In general, the degree of dispersion of the clay platelets into the polymer matrix determines the structure of nanocomposites. Depending on the interaction between the clay and the polymer matrix, two main idealized types of polymer–clay morphologies can be obtained: namely, intercalated and exfoliated. The intercalated structure results from penetration of a single polymer chain into the galleries between the silicate layers, resulting in formation of alternate layers of polymer and inorganic layers. An exfoliated structure results when the individual silicate layers are completely separated and dispersed randomly in a polymer matrix. Usually exfoliated nanocomposites are preferred because they provide the best property improvements [36]. The preparation of clay-based nanocomposites is achieved by several methods: melt intercalation, solution exfoliation, and *in situ* polymerization. In the *in situ* polymerization method, the monomer is used directly as a solubilizer for swelling the layered silicate. Polymerization occurs in the intercalated clays [37-40].

Since the remarkable improvements in the material properties in a nylon-6/clay nanocomposite demonstrated by the Toyota research group [41] numerous other polymers have been investigated by many researchers around the World. These include, but are not limited to, polypropylene, polyethylene, polystyrene, poly(ethylene oxide), polycaprolactone, polyimides, polyamides, poly(ethylene terephthalate), polycarbonate, polyurethane, poly(thiophene), polybenzimidazole, poly(pyrrole) and epoxy resins [21-24, 39, 40, 42-52].

2-thiozyl methacrylamide (TMAAm) is one of the most important vinyl monomers for large polymer-add-on can be easily obtained because of the hydrophilic natüre of the TMAAm [53, 54]. Poly(2-thiozyl methacrylamide), as an important industrial polymer, has some desirable properties, including, it is less toxic, polar and less expensive than other vinyl monomers [55]. Polymers based on methacrylamide with very high molecular weights have gained more and more technical attention due to the solubility in water. However, its biggest disadvantage is poor thermal and mechanical properties. Therefore, TMAAm-VBOA/MMT nanocomposites offer the especially thermal stability.

The aim of this study is to exhibit the preparation and characterization of TMAAm-VBOA/MMT nanocomposites. The nanocomposites prepared were characterized by Fourier Traansform Infrared Spectroscopy (FTIR), X-ray diffraction (XRD), scanning electron microscopy (SEM), and thermogravimetric analysis (TGA). Also, we investigated the pore size properties of nanocomposites by using BET analysis.

2. EXPERIMENTAL DATAILS

2.1. Reagents

2-aminothiazole, methacryloyl chloride and triethylamine (Sigma-Aldrich) was used as received. Benzoyl peroxide (Bz_2O_2) (Merck) was purified by successive crystallizations from chloroform- methanol mixture. 4-vinylbenzyl chloride (Sigma-Aldrich), N,N-dimethyloctadecylamine (Sigma-Aldrich), 1,4-dioxane, N,N-dimethylformamide, dichloromethane, methanol (Merck), were analytical grade commercial products and used as received. 2-Thiozyl methacrylamide was synthesized as pursuant to the literatüre [41]. The sodium montmorillonite clay, with a cation exchange capacity 1.08 mol kg^{-1}, was obtained from Reşadiye (Tokat/Turkey). It was used after further purification [56]. It was named as Na-MMT.

2.2. Methods of Characterization

^{1}H-and ^{13}C-NMR spectra of the polymers were recorded in $CDCl_3$ with tetramethylsilane as the internal standard using a Bruker 400 MHz NMR instrument. Fourier transform infrared (FTIR) spectra were done by Perkin-Elmer spectrum two spectrometer. The microstructure of the nanocomposites were examined by a scanning electron microscopy (SEM), Leo 440, Model:JSM-5600 imaging mode. The BET surface area and porosity of the nanocomposites were determined by the BET-N_2 method using a Micromeritics Gemini VII analyzer. The sample was degassed at 80 ^{o}C for 12 h. Thermal data were obtained by using a Perkin Elmer Diamond TG-DTA thermobalance in N_2 atmosphere. XRD study of the nanocomposites was performed on a Rıgaku Dmax2200 XRD Model X powder diffractometer, using CoKα radiation whose wavelength was 0,178901 nm, and a Ni filter was used.

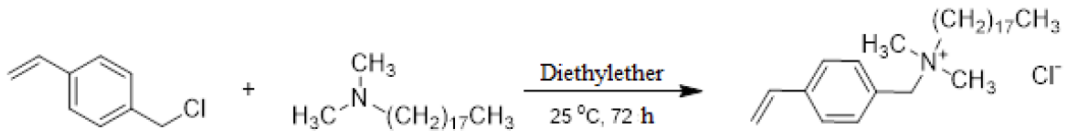

Scheme 1: Synthesis route of VBOAC.

2.3. Vinylbenzyldimethyloctadecyl Ammonium Chloride (VBOAC) Synthesis

N-N-dimethyloctadecylamine and 4-vinylbenzyl chloride was used for the VBOAC synthesis. In this investigation, VBOAC is synthesized through the reaction between 4-vinylbenzyl chloride and N,N-dimethyloctadecyl amine. Firstly, 20.83 g (0.070 mol) dimethyloctadecylamine was dissolved in 150 mL diethylether. After then, 11.5 mL (0.070 mol) 4-vinylbenzyl chloride was added to this solution for 48 h. The resulting precipitate was filtered and washed with ethylacetate. The resulting crystals were dried at room temperature. The reaction equation is shown in Scheme **1**.

2.4. Vinylbenzyldimethyloctadecylammonium/ Montmorillonite (VBOA/MMT) Synthesis

VBOAC was used for the synthesis of VBOA/MMT by the well-known ion exchange method. Firstly 8.5 g (7.88 mmol) clay (Na-MMT) was dispersed in 400 mL ultra-pure water for 48 h and pH of solution was adjusted to 3 with concentrated HCl. 7.7 g (11.11 mmol) VBOAC was added to solution more than CEC value of value of Na-MMT and mixed with magnetic stirrer at 500 rpm for 24 h. After preparation of VBOA/MMT, sample was washed for several times and centrifuged at 4000 rpm. VBOA/MMT was dried at 40 ^{o}C . The reaction equation is shown in Scheme **2**.

2.5 Monomer Synthesis

To a well-stirred solution of 30 mmole 2-Aminothiazole and 90 mmole of triethylamine (NR_3) in 30 ml dichloromethane, 30 mmole of methacryloylchloride was added dropwise under cooling in ice bath (0-5 ^{o}C). After the complete addition of methacryloyl chloride, the reaction mixture was stirred for 12 h at room temperature, then filtered and evaporated with a rotavapour. A yellow product was obtained and recrystallized from ethanol as a yellow powder (yield 85%). The reaction equation is shown in Scheme **3**.

2.6. Preparation of TMAAm-VBOA/MMT Nanocomposites

The desired amount of VBOA/MMT in distilled water was dispersed overnight. Then, at suitable concentration TMAAm and Bz_2O_2 as radical initiator (dissolved in 1 mL acetone) were added upon the dispersion. The samples were polymerized in a water bath adjusted to the polymerization temperature (80

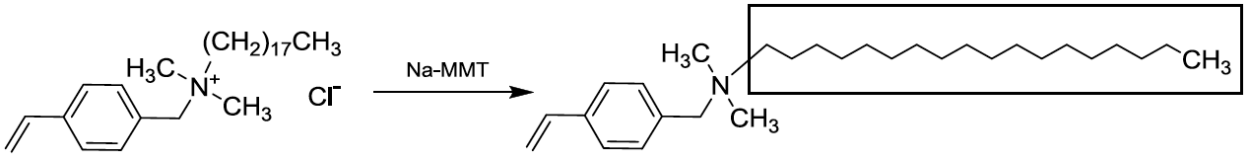

Scheme 2: Synthesis route of VBOA/MMT.

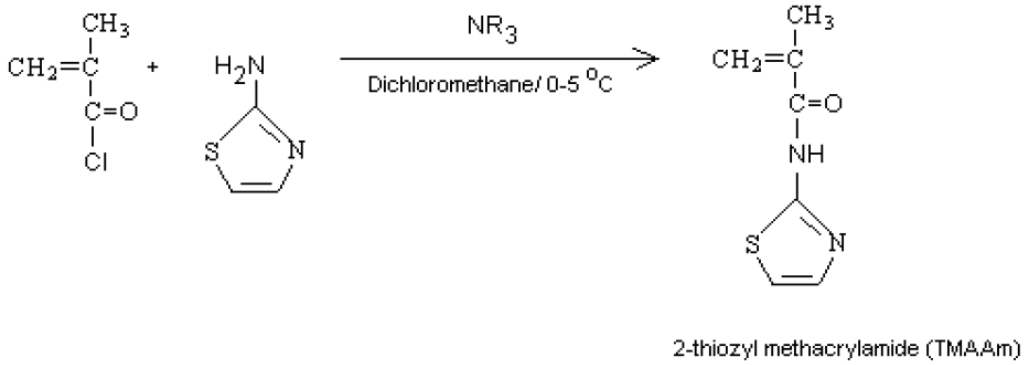

Scheme 3: Synthesis route of TMAAm monomer.

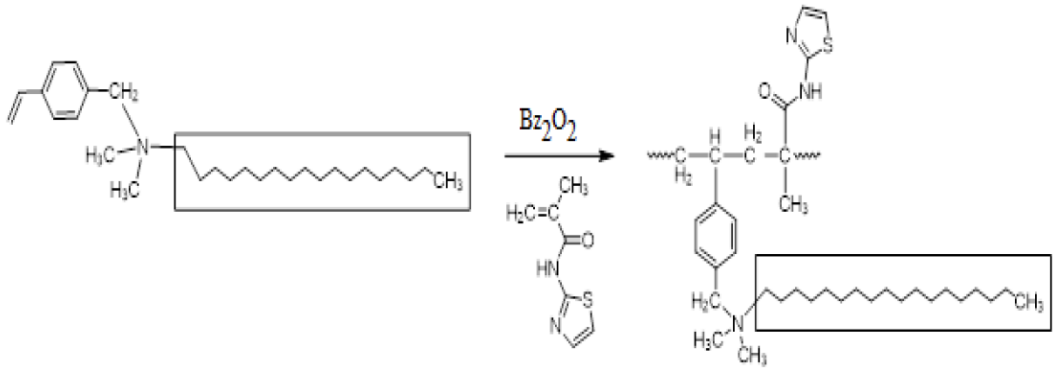

Scheme 4: Preparation of nanocomposites.

Table 1: Codes and Chemical Compositions of Samples and Polymerization Conditions

Sample code	Monomer content (wt%)[a]	VBHA/MMT content (wt%)[b]
Pure Na-MMT	-	100.00
TMAAm-VBHA/MMT1	50.00	50.00
TMAAm-VBHA/MMT2	66.67	33.33
TMAAm-VBHA/MMT3	75.00	25.00
Pure TMAAm	100.00	-

Bz_2O_2 concentration = 3.0 x 10^{-3} mol/L, temperature = 80 ^oC, time = 2 h.
[a]Calculated by dividing the weight of TMAAm by the weight of (VBHA/MMT + monomer).
[b]Calculated by dividing the weight of VBHA/MMT by the weight of (VBHA/MMT + monomer).

^oC) for 2 h to obtain TMAAm-VBOA/MMT nanocomposites. The reaction of nanocomposite preparation is shown in Scheme **4**.

After polymerization, obtained nanocomposites were washed througly with distilled water. The nanocomposites were then dried overnight in a vacuum oven at 40 ^oC and weighed. The other samples were prepared by the same procedure using different concentrations of TMAAm. Codes and compositions of samples and the polymerization conditions are listed in Table **1**.

3. RESULTS AND DISCUSSION

3.1. FTIR Characterization

The FT-IR spectra of TMAAm, VBOAC, VBOA/MMT and different composition of TMAAm-VBOA/MMT nanocomposite are shown in Figure **1a-b**.

Both püre TMAAm and TMAAm-VBOA/MMT nanocomposites have characteristic bands of poly 2-thiozyl methacrylamide: NH stretching band at 3206-3362 cm^{-1}. A strong band at 3011 cm^{-1} is due to C–H in the aromatic and thiazole ring. The asymmetrical and symmetrical stretchings of methyl and methylene groups are observed at 2924, 2900 and 2860 cm^{-1}, respectively. C=O amide peaks at 1668 cm^{-1}, and CN stretching band is at 1620 cm^{-1}. Besides these bands, TMAAm-VBOA/MMT nanocomposite also has the characteristic bands of VBOA/MMT: 1040, 525 and 470 cm^{-1}, which correspond to the stretching band of Si-O, the deformation band of Si-O-Al and the Si-O-Si deformation band of VBOA/MMT. These indicated that TMAAm chains stay immobilized inside and/or on the clay layers [57]. In other words, VBOA/MMT has been incorporated in TMAAm matrix.

3.2. X-Ray Diffraction Spectroscopy

By studying the XRD pattern of the nanocomposites the presence of TMAAm in the composite can be further confirmed. XRD spectra of the püre Na-MMT and nanocomposites with different monomer contents are shown in Figure **2**.

The *d*-spacing values (d_{001}) of the pure Na-MMT and nanocomposite samples were calculated by using the Bragg equation, $d = \lambda/2 \sin\theta$, and shown beside each peak. Also, the obtained results are presented in Table **2**.

On the XRD spectra, it can be seen that the (d_{001}) spacing of püre Na-MMT was 1.20 nm after vacuum

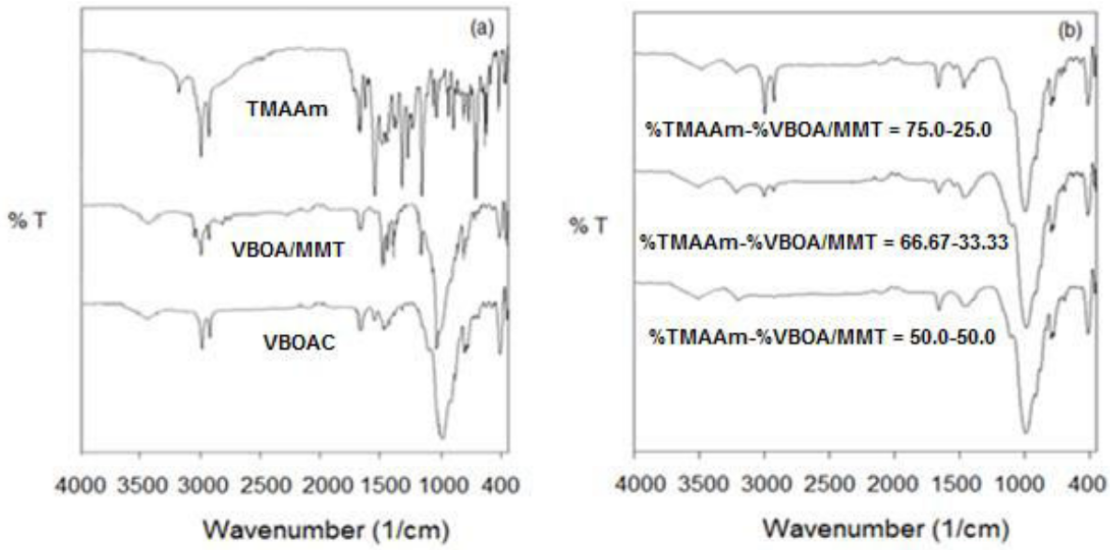

Figure 1: FTIR spectra of (a) TMAAm monomer, VBOAC, VBOA/MMT and (b) TMAAm-VBOA/MMT nanocomposites.

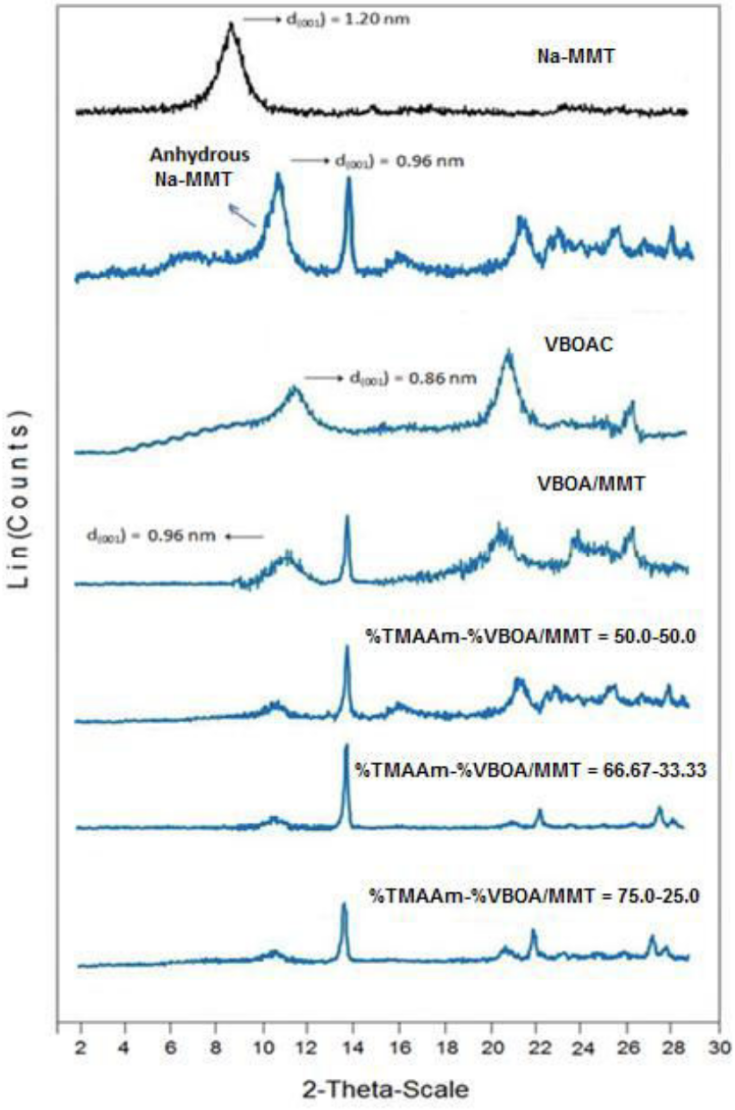

Figure 2: XRD pattern of the Na-MMT, VBOAC, VBOA/MMT and TMAAm-VBOA/MMT nanocomposites.

Table 2: d(001) Values and Structure of Na-MMT, VBHAC, VBHA/MMT and TMAAm-VBHA/MMT Nanocomposites

Sample No	2θ (°)	d_{001} (nm)	Structure
Na-MMT	8,6	1,20	-
Anhydrous Na-MMT	10,8	0,96	-
VBHAC	11,8	0,86	-
VBHA/MMT	10,7	0,96	-
TMAAm-VBHA/MMT1	-	-	Exfoliated
TMAAm-VBHA/MMT2	-	-	Exfoliated
TMAAm-VBHA/MMT3	-	-	Exfoliated

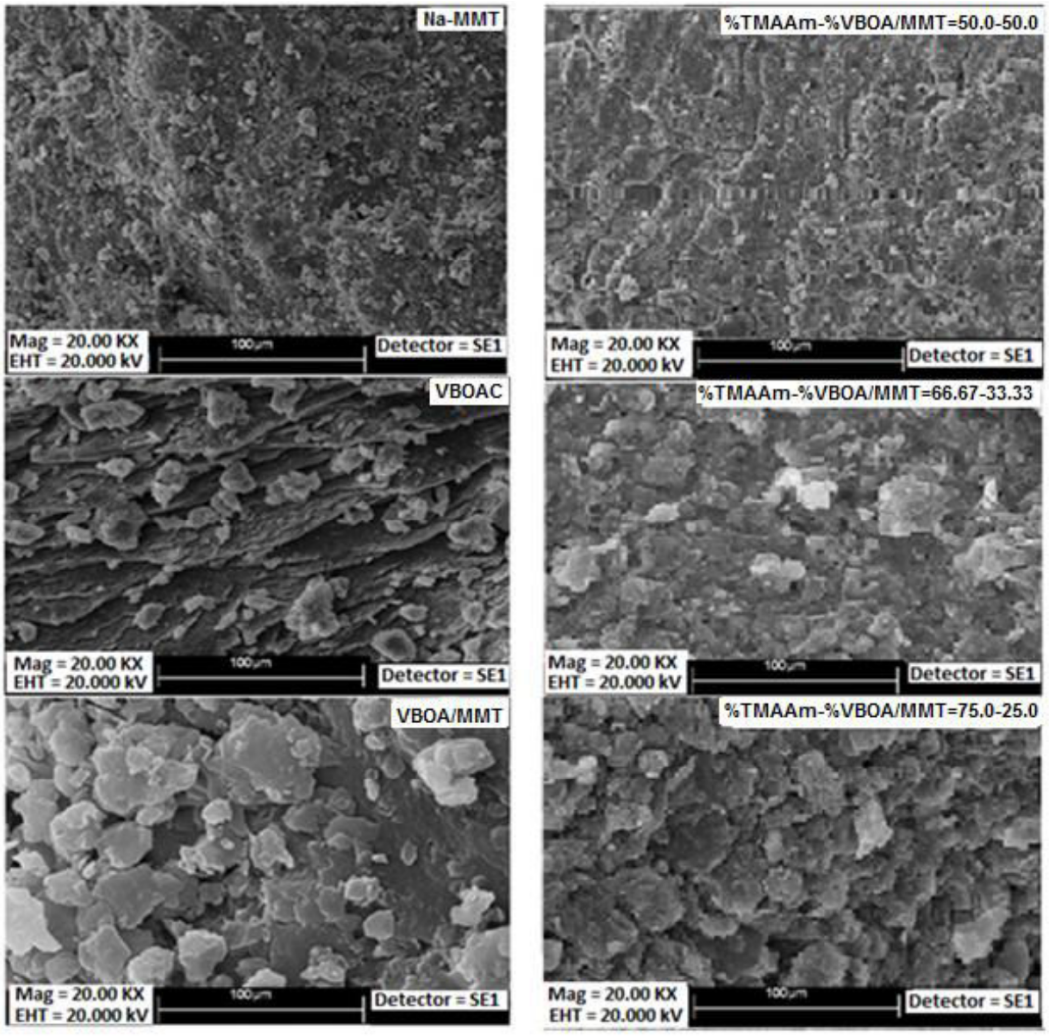

Figure 3: SEM micrographs of the Na-MMT, VBOAC, VBOA/MMT and TMAAm-VBOA/MMT nanocomposites.

drying and, after polymerization process. 1 nm-thick the individual clay layers are dispersed in a continuous polymer matrix by an average distances that depends on clay loading, these results suggest that an exfoliated nanocomposite. Usually, the clay content of an exfoliated nanocomposite is much lower than that of an intercalated nanocomposite. The latter configuration is of particular interest because it maximizes the polymer-clay interactions, making the entire surface of the layers available for the polymer. This is direct evidence that polymer chains have been exfoliated in the clay layers and exfoliated TMAAm-VBOA/MMT nanocomposite has been synthesized.

3.3. Morphological Dissimilarities of Nanostructures

Scanning electron microscopy (SEM) was used for further characterization and observes the morphology of the püre Na-MMT, VBOAC, VBOA/MMT, and TMAAm-VBOA/MMT nanocomposites. The results are illustrated in Figure **3**.

Pure Na-MMT shows individual layers of the clay. In TMAAm-VBOA/MMT nanocomposite images, it can be seen that the clay layers are dispersed homogeneously in the polymer matrix and the interlayer spacing of VBOA/MMT is expanded, which is evidence for the exsfoliated morphology [58]. This agrees well with XRD observations.

3.4. Thermo-Physical Property of Nanocomposites

The thermogravimetric analysis of TMAAm, VBOAC, VBOA/MMT and TMAAm-VBOA/MMT nanocomposite containing 66.67 wt% TMAAm monomer was performed and results are shown in Figure **4**.

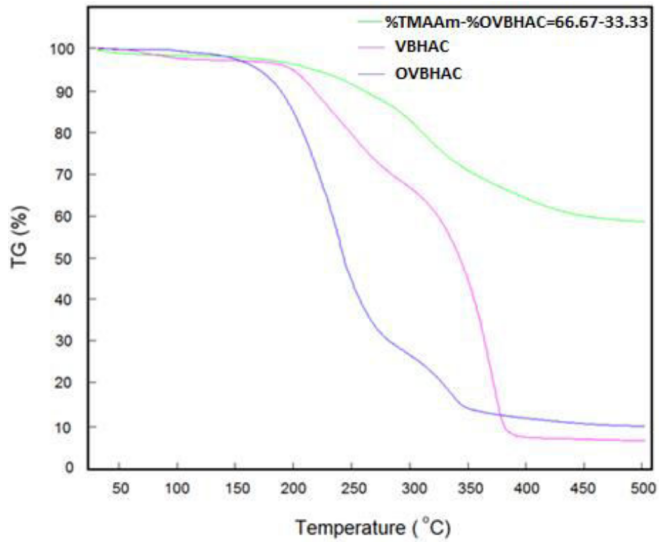

Figure 4: TGA curves of the VBOAC, VBOA/MMT and TMAAm-VBOA/MMT (66.67-33.33) nanocomposite.

Thermal degradation of TMAAm was performed by two steps. The weight loss of the first step was found to be 65% between 150-260 ^{o}C. The weight loss of the second step was found to be 18% between 260-340 ^{o}C and the total weight loss is 85% up to 500 ^{o}C. The TGA curve of VBOAC indicates that there is a one stage of decomposition. The total weight loss of 83% between 160-360 ^{o}C. The TGA curve of VBOA/MMT indicates that there are two stages of decomposition. The weight loss of the first step was found to be 28% between 200-320 ^{o}C. The weight loss of the second step was found to be 12% between 320-500 ^{o}C. The total weight loss is 40% up to 500 ^{o}C. As could be expected, the TMAAm-VBOA/MMT shows a high thermal stability. The TGA curve of TMAAm-VBOA/MMT (66.67 wt% TMAAm) nanocomposite indicates that there are two stages of decomposition. The first one is small and occurred between 190-280 ^{o}C. The second stage is the thermal decomposition of exsfoliated nanocomposite. İts weight loss reaches 93% at 500 ^{o}C. With regard to the second stage, the TMAAm-VBOA/MMT nanocomposite has a higher decomposition temperature than püre TMAAm. This enhancement in the thermal stability is due to the presence of clay nanolayers with high thermal stability and the great barrier properties of the nanolayers dispersed in the nanocomposites to maximize the heat insulation [58,59]. Also, it can be attributed to the introduction of VBOA/MMT layers into the TMAAm matrix and finally intercalation with VBOA/MMT which can greatly improve the thermal stability of TMAAm. This result is consistent with the reports by many other researchers [60,61].

3.5. BET Analyses of Materials

BET analysis method was used to determine surface area and pore size distribution of VBOAC, VBOA / MMT and TMAAm-VBOA / MMT nanocomposites. Curves of N_2 adsorption-desorption isotherms for the TMAAm-VBOA / MMT1 synthesized nanocomposites are shown in Figure **5**.

The corrected relative pressure values (P/P_o) were obtained by continuously monitoring N_2 saturation pressure during the measurement. Where P is the equilibrium pressure and P_o is the saturation pressure of N_2 at the measuring temperature. According to Dubinin propasal [62] and later adopted by IUPAC [63], the pore sizes can be classified: pore sizes for macropores (larger than 500 Å), mesopores (between 20 and 500 Å), and micropores of less than 20 Å. By using the BET equation [64] the Brauner-Emmet-Teller (BET) specific surface area (SBET) was calculated. Pore Size Distribution (PSD) curve derived from the desorption branch of the isotherm is likely to give a misleading picture of the pore structure in particular the size distribution will appear to be much narrower than it actually is [63]. Pore volume was measured during the analysis and PSD of vacuum getter was estimated by the Barrett-Joyner-Halenda (BJH) method within the pore diameter range from 1.50 nm to about 900 nm [65]. By assuming that the pores were then filled with condensed adsorptive in the normal liquid state. The

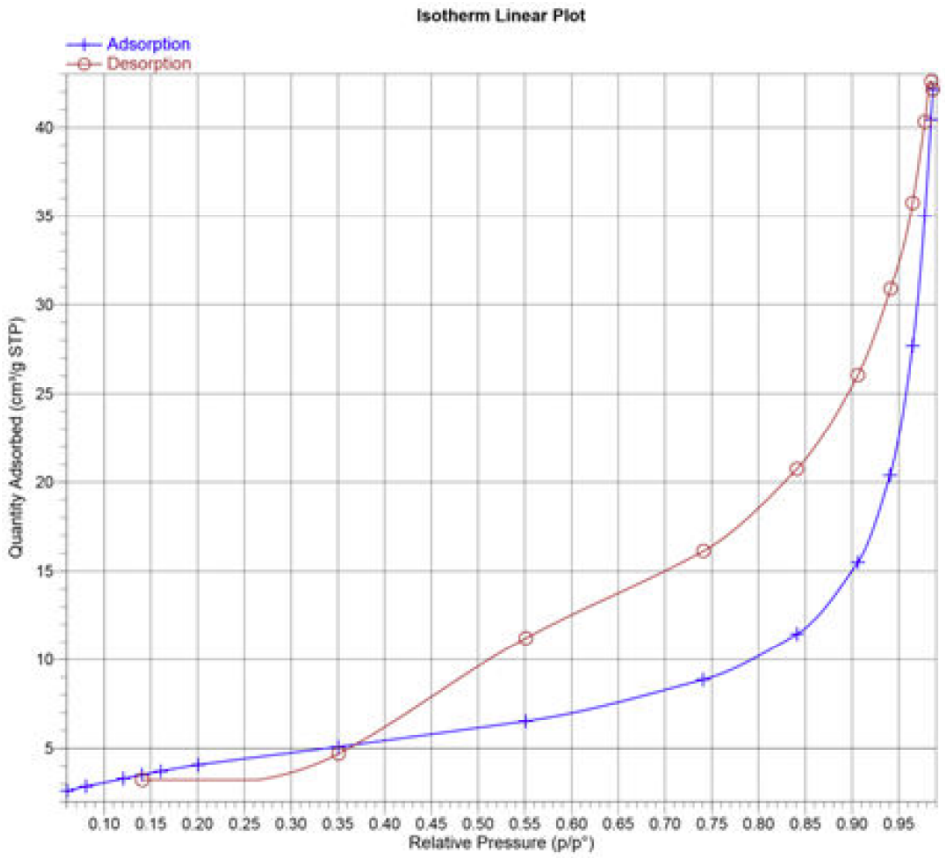

Figure 5: The N_2 adsorption-desorption isotherms for the TMAAm-VBOA/MMT1 nanocomposite.

total pore volume was derived from the amount of gas adsorbed at a relative pressure close to unity.

As can be seen in Figure **5**. there are two sharp increases. The first one is observed at P/P_o of 0.060, suggesting the presence of micropores. The second abrupt increase in the adsorption capacity shown in the neighborhood at P/P_o of 0.75. This is due to the continuous progression from multilayer adsorption to capillary condensation in which the smaller pores become completely filled with liquid nitrogen. This occurs because the saturation vapor pressure in a small pore is reduced according to Kelvin equation [63,66], by the effect of surface tension. When P/P_o is higher than 0.94, the adsorption capacity hardly decreases and that very pores with a but diameter exist. TMAAm-VBOA/MMT (50.00 VBOA/MMT) nanocomposite vacuum getter shows a saturated adsorption capacity of 40.0 cm^3(STP)/g at P/P_o=0.99. The adsorption isotherm corresponds to type IV of the IUPAC classification in the range P/P_o of 0.14e 0.99 is observed, which represents the macroporous structural characteristic. Pore size distributions of nanocomposites vacuum getter which were calculated from both branches of the hysteresis loop by the BJH method. Also, the obtained results are presented in Table **3**.

Table 3: BET Results of VBHAC, VBHA/MMT and TMAAm-VBHA/MMT Nanocomposites

Sample No	BET Surface Area (m^2/g)	BJH Adsorption Pore Volume (cm^3/g)	BJH Desorption Pore Volume (cm^3/g)	Adsorption Pore Size (nm)	Desorption Pore Size (nm)
VBHAC	0.1443	0.002894	0.002874	71.4522	81.95243
VBHA/MMT	1.8370	0.027552	0.028511	56.26529	61.98388
TMAAm-VBHA/MMT1	0.9870	0.020289	0.026282	77.28174	106.25332
TMAAm-VBHA/MMT2	0.3634	0.005227	0.005401	53.91921	59.16581
TMAAm-VBHA/MMT3	0.1687	0.002813	0.002820	60.76366	65.95766

Average pore diameter denoted the pores are mostly macropores. Macropores is generally useful for liquid-solid adsorption [67].

CONCLUSIONS

Vinylbenzyldimethyloctadecylammonium montmorillonite (VBOA/MMT), a cationic surfactant with a polymerizable group was synthesized for the preparation of VBOAC and Na-MMT. This surfactant copolymerizes with 2-thiozyl methacrylamide. Exfoliated 2-thiozyl methacrylamide nanocomposites were succesfully synthesized by free radical polymerization using functionalized forms of VBOA/MMT. Recent advancements in material technologies have promoted the development of various preparation strategies and applications of novel polymer–nanoclay composites. Innovative synthesis pathways have resulted in novel polymer–nanoclay composites with improved properties, which have been successfully incorporated in diverse fields such as aerospace, automobile, construction, petroleum, biomedical and wastewater treatment. These composites are recognized as promising advanced materials due to their superior properties, such as enhanced density, strength, relatively large surface areas, high elastic modulus, flame retardancy, and thermomechanical/optoelectronic/magnetic properties. There are three major synthesis procedures for polymer/nanoclay composites including the solution-blending method, melt-blending method and *in-situ* polymerization method . Until now, the most broadly applied synthesis method was the *in-situ* polymerization method, where the grafted amounts of organics was adjusted and the clay interlayer spacing was controlled by changing the polymerization conditions. The combination of *in-situ* polymerization with efficient coupling methods, including click chemistry, radical-mediated polymerization, tandem preparation, photopolymerization and miniemulsion has enabled effective dispersion of nanoclays in the form of individual platelets in the polymer matrix, which is a significant challenge inherent to the synthesis of polymer/nanoclay composites. All these methods have been successfully implemented for the chemical modification of clay surfaces with low molecular or polymeric grafts. Approximately 75–80% of the polymer/nanoclay composites are implemented in the automotive, aeronautical, and packaging industries. Companies are investing billions of dollars per annum in developing novel polymer/nanoclay composite materialsCompared to solution blending methods, ultrasound-assisted *in-situ* polymerization resulted in composites with improved reaction time, clay dispersion and composite yield. Based on the silicate dispersion data, *in-situ* polymerization is more effective in the formation of composites, and can bypass the rigorous thermodynamic requirements associated with the polymer intercalation process. Moreover, *in-situ* polymerization allows versatile molecular designs of the polymer matrix; it delivers an effective approach to the synthesis of different polymer/nanoclay composites with an expanded property range and enables the design of the interface between the nanoclays and the polymers by flexible tuning of the matrix composition and structure [6]. TMAAm-VBOA/MMT nanocomposites show a higher thermal degradation temperature than püre VBOA/MMT and poly(TMAAm). The SEM micrographs provided exfoliated polymer chains within the clay layers.

ACKNOWLEDGEMENTS

This study was funded by Uşak University Research Fund (Project no: 2014/TP007).

CONFLICT OF INTEREST

The authors declare that they have no conflict of interest.

REFERENCES

[1] Kojima Y, Usuki A, Kawasumi M, Okada A, Fukushima Y, Kurauchi T, Kamigaito O. Mechanical Properties of Nylon 6-Clay Hybrid. Journal of Materials Research 1993; 8(5): 1185. https://doi.org/10.1557/JMR.1993.1185

[2] Kojima Y, Usuki A, Kawasumi M, Okada A, Kurauchi T, Kamigaito O. Synthesis of Nylon 6–Clay Hybrid by Montmorillonite Intercalated with ϵ -Caprolactam. Journal of Polymer Science, Part A: Polymer Chemistry 1993; 31(4): 983. https://doi.org/10.1002/pola.1993.080310418

[3] Liu LM, Qi ZN, Zhu XG. Studies on Nylon-6 Clay Nanocomposites by Melt-Intercalation Process. Journal of Applied Polymer Science 1999; 71(7): 1133. https://doi.org/10.1002/(SICI)1097-4628(19990214)71:7%3C1133::AID-APP11%3E3.0.CO;2-N

[4] Lan T, Kaviratna PD, Pinnavaia TJ. On the Nature of Polyimide-Clay Hybrid Composites. Chemistry Materials 1994; 6(5): 573. https://doi.org/10.1021/cm00041a002

[5] Quang TN, Donald GB. Preparation of Polymer–Clay Nanocomposites and Their Properties. Advanced Polymer Technology 2006; 25(4): 270. https://doi.org/10.1002/adv.20079

[6] Guo F, Aryana S , Han Y, Jiao Y. A Review of the Synthesis and Applications of Polymer–Nanoclay Composites. Applied Sciences 2018; 8: 1696 http://dx.doi.org/10.3390/app8091696

[7] Cherifi N, BenAboura A, Save M, Billon L. Acrylic Diblock Copolymers/Clay Nanocomposites Via In situ Nitroxide Mediated Polymerization. Macromolecular Chemistry and Physics 2015; 216: 1462. https://doi.org/10.1002/macp.201500076

[8] Liu L, Wei SL, Lai XJ. In situ Synthesis and Characterization of Polypropylene/Polyvinyl acetate-Organophilic Montmorillonite Nanocomposite. Journal of Applied Polymer Science 2012; 124(5): 4107. https://doi.org/10.1002/app.35210

[9] Zhao LJ, Li J, Guo SY, Du Q. Ultrasonic Oscillations Induced Morphology and Property Development of Polypropylene/ Montmorillonite Nanocomposites. Polymer 2006; 47(7): 2460. https://doi.org/10.1016/j.polymer.2006.02.011

[10] Abe A, Albertsson AC, Cantow HJ, Dusek K, Edwards S, Hocker H, Joanny JF, Kausch HH, Kobayashi T, Lee KS, McGrath JE, Monnerie L, Stupp SI, Suter UW, Wegner G, Young RJ. New Polymerization Techniques And Synthetic Methodologies. Book Series: Advances in Polymer Science 2001; 155: 167-221.

[11] Abbasian M, Pakzad M, Amirmanesh M. Polymericaly Modified Clays to Preparation of Polystyrene Nanocomposite by Nitroxide Mediated Radical Polymerization and Solution Blending Methods. Polymer Composites 2017; 38(6): 1127. https://doi.org/10.1002/pc.23675

[12] Abedi S, Abdouss M. A Review of Clay-Supported Ziegler-Natta Catalysts for Production of Polyolefin/Clay Nanocomposites Through In situ Polymerization. Applied Catalysis A-General 2014; 475:386. https://doi.org/10.1016/j.apcata.2014.01.028

[13] Albdiry MT, Yousif BF, Ku H, Lau KT. A Critical Review on the Manufacturing Processes in Relation to the Properties of Nanoclay/Polymer Composites. Journal of Composite Materials 2013; 47(9): 1093. https://doi.org/10.1177/0021998312445592

[14] Asensio M, Herrero M, Nunez K, Gallego R, Merino JC, Pastor JM. In situ Polymerization of Isotactic Polypropylene Sepiolite Nanocomposites and Its Copolymers by Metallo-cene Catalysis. European Polymer Journal 2018; 100: 278. https://doi.org/10.1016/j.eurpolymj.2018.01.034

[15] Atta AM, Al-Lohedan HA, Ezzat AO, Issa ZA, Oumi AB. Synthesis and Application of Magnetite Polyacrylamide Amino-Amidoxime Nano-Composites as Aadsorbents for Water Pollutants. Journal of Polymer Research 2016; 23(4): 1. https://doi.org/10.1007/s10965-016-0963-z

[16] Boukoussa B, Abidallah F, Abid Z, Talha Z, Taybi N, El Hadj HS, Ghezini R, Hamacha R, Bengueddach A. Synthesis of Polypyrrole/Fe-Kanemite Nanocomposite Through In situ Polymerization: Effect of Iron Exchange, Acid Treatment, and CO2 Aadsorption Properties. Journal of Materials Science 2017; 52(5): 2460. https://doi.org/10.1007/s10853-016-0541-0

[17] Burmistr MV, Sukhyy KM, Shilov VV, Pissis P, Spanoudaki A, Sukha IV, Tomilo VI, Gomza YP. Synthesis, Structure, Thermal and Mechanical Properties of Nanocomposites Based on Linear Polymers and Layered Silicates Modified by Polymeric Quaternary Ammonium Salts (ionenes). Polymer 2005; 46(26): 12226. https://doi.org/10.1016/j.polymer.2005.10.094

[18] Buruga K, Kalathi JT. A Facile Synthesis of Halloysite Nanotubes Based Polymer Nanocomposites for Glass Coating Application. Journal of Alloys and Compounds 2018; 735: 1807. https://doi.org/10.1016/j.jallcom.2017.11.211

[19] Cardoso RS, Aguiar VO, Marques MDV. Masterbatches of Polypropylene/Clay Obtained by In situ Polymerization and Melt-Blended with Commercial Polypropylene. Journal of Composite Materials 2017; 51(25): 3547. https://doi.org/10.1177/0021998317690444

[20] Fornes TD, Yoon PJ, Keskkula H, Paul DR. Nylon-6 Nanocomposites: The Effect of Matrix Molecular Weight. Polymer 2001; 42(25): 9929. https://doi.org/10.1016/S0032-3861(01)00552-3

[21] Doh JG, Cho I. Synthesis and Properties of Polystyrene-Organoammonium Montmorillonite Hybrid. Polymer Bulletin 1998; 41(5): 511. https://doi.org/10.1007/s002890050395

[22] Chieng BW, Ibrahim NA, Wan Yunus WMZ. Effect of Organo-Modified Montmorillonite on Poly(Butylene Succinate)/Poly(Butylene Adipate-co-Terephthalate) Nanocomposites. Express Polymer Letters 2010; 4(7): 404. https://doi.org/10.3144/expresspolymlett.2010.51

[23] Cheng HY, Weng CJ, Liou SJ, Yeh JM, Liu SP. Studies on Heterogeneous Nucleation Effect of Dispersing Intercalated Montmorillonite Clay Platelets in Polyaniline Matrix. Polymer Composite 2010; 31(12): 2049. https://doi.org/10.1002/pc.21003

[24] Mansoori Y, Atghia SV, Zamanloo MR, İmanzadeh GH, Sirousazar M. Polymer–Clay Nanocomposites: Free-Radical Grafting of Polyacrylamide onto Organophilic Montmorillonite. European Polymer Journal 2010; 46(9): 1844. https://doi.org/10.1016/j.eurpolymj.2010.07.006

[25] LeBaron PC, Wang Z, Pinnavaia TJ. Polymer-Layered Silicate Nanocomposites: An Overview. Applied Clay Science 1999; 15(1-2): 11. https://doi.org/10.1016/S0169-1317(99)00017-4

[26] Kim DV, Kumar J, Blumstein A. Ordered Assembly of Conjugated Ionic Polyacetylenes within Clay Nanoplatelets: Layer-by-Layer Assembly and Intercalative Polymerization. Applied Clay Science 2005; 30(2): 134. https://doi.org/10.1016/j.clay.2005.04.005

[27] Theng BKG. Formation and Properties of Clay–Polymer Complexes, Elsevier: Amsterdam, 1979.

[28] Krishnamoorti R, Vaia RA, Giannelis EP. Structure and Dynamics of Polymer-Layered Silicate Nanocomposites. Chemistry Materials 1996; 8(8): 1728. https://doi.org/10.1021/cm960127g

[29] Vaia RA, Price G, Ruth PN, Nguyen HT, Lichtenhan J. Polymer/Layered Silicate Nanocomposites as High Performance Ablative Materials. Applied Clay Science 1999; 15(1-2): 67. https://doi.org/10.1016/S0169-1317(99)00013-7

[30] Biswas M, Sinha SR. Recent Progress in Synthesis and Evaluation of Polymer Montmorillonite Nanocomposites. Advanced Polymer Science 2001; 155: 167. https://doi.org/10.1007/3-540-44473-4-3

[31] Messersmith PB, Giannelis EP. Synthesis and Barrier Properties of Poly(ε-Capro1actone)-Layered Silicate Nanocomposites. Journal of Polymer Science, Part A: Polymer Chemistry 1995; 33(7): 1047. https://doi.org/10.1002/pola.1995.080330707

[32] Giannelis P. Polymer-Layered Silicate Nanocomposites: Synthesis, Properties and Applications. Applied Organometal Chemistry 1998; 12(10-11): 675. https://doi.org/10.1002/(SICI)1099-0739(199810/11)12:10/11<675::AID-AOC779>3.0.CO;2-V

[33] Gilman JW. Flammability and Thermal Stability Studies of Polymer Layered-Silicate (Clay) Nanocomposites. Applied Clay Science 1999; 15(1-2): 31. https://doi.org/10.1016/S0169-1317(99)00019-8

[34] Lan T, Kaviratna PD, Pinnavaia TJ. On the Natüre of Polyimide Clay Hybrid Composites. Chemistry Materials 1994; 6(5): 573. https://doi.org/10.1021/cm00041a002

[35] Bourbigot S, LeBras M, Dabrowski F, Gilman JW, Kashiwagi T. PA-6 Clay Nanocomposite Hybrid as Char Forming Agent in Intumescent Formulations. Fire Materials 2000; 24(4): 201. https://doi.org/10.1002/1099-1018(200007/08)24:4<201::AID-FAM739>3.0.CO;2-D

[36] Masenelli-Varlot K, Reynaud E, Vigier G, Varlet J. Mechanical Properties of Clay-Reinforced Polyamide.

Journal of Polymer Science, Part B: Polymer Physics 2002; 40: 272. https://doi.org/10.1002/polb.10088

[37] Ray SS, Okamoto M. Polymer/Layered Silicate Nanocomposites: A Review From Preparation to Processing. Progres in Polymer Science 2003; 28(11): 1539. https://doi.org/10.1016/j.progpolymsci.2003.08.002

[38] Nguyen QT, Baird DG. Preparation of Polymer–Clay Nanocomposites and Their Properties. Advanced Polymer Technology 2006; 25(4): 270. https://doi.org/10.1002/adv.20079

[39] Jaymand M. Surface Modification of Montmorillonite with Novel Modifier and Preparation of Polystyrene/ Montmorillonite Nanocomposite by In situ Radical Polymerization. Journal of Polymer Research 2011; 18(5): 957. https://doi.org/10.1007/s10965-010-9495-0

[40] Yenice Z, Taşdelen AM, Oral A, Güler C, Yağcı Y. Poly(Styrene-b-Tetrahydrofuran)/Clay Nanocomposites by Mechanistic Transformation. Journal of Polymer Science, Part A:Polymer Chemistry 2009; 47(8): 2190. https://doi.org/10.1002/pola.23332

[41] Okada A, Fukoshima Y, Inagaki S, Usuki A, Sugiyama S, Kurashi T, Kamigaito O. U.S. Patent 4,739,007, 1998.

[42] Kato M, Usuki A, Okada A. Synthesis of Polypropylene Oligomer–Clay Intercalation Compounds. Journal of Applied Polymer Science 1997; 66(9): 1781. https://doi.org/10.1002/(SICI)1097-4628(19971128)66:9<1781::AID-APP17>3.0.CO;2-Y

[43] Kawasumi M, Hasegawa N, Kato M, Usuki A, Okada A. Preparation and Mechanical Properties of Polypropylene-Clay Hybrids. Macromolecules 1997; 30(20): 6333. https://doi.org/10.1021/ma961786h

[44] Hasegawa N, Kawasumi M, Kato M, Usuki A, Okada A. Preparation and Mechanical Properties of Polypropylene-Clay Hybrids Using a Maleic Anhydride-Modified Polypropylene Oligomer. Journal of Applied Polymer Science 1998; 67(1): 87. https://doi.org/10.1002/(SICI)1097-4628(19980103)67:1<87::AID-APP10>3.0.CO;2-2

[45] Liu X, Wu Q. PP/Clay Nanocomposites Prepared by Grafting-Melt Intercalation. Polymer 2001; 42(25): 10013. https://doi.org/10.1016/S0032-3861(01)00561-4

[46] Nam PH, Maiti P, Okamoto M, Kotaka T, Hasegawa N, Usuki A. A Hierarchical Structure and Properties of Intercalated Polypropylene/Clay Nanocomposites. Polymer 2001; 42(23): 9633. https://doi.org/10.1016/S0032-3861(01)00512-2

[47] Privalko VP, Calleja FJB, Sukhorukov DI, Privalko EG, Walter R, Friedrich K. Composition-Dependent Properties of Polyethylene/Kaolin Composites - Part II - Thermoelastic Behaviour of Blow-Moulded Samples. Journal of Materials Science 1999; 34(3): 497. https://doi.org/10.1023/A:1004586427045

[48] Alexandre M, Dubois P, Sun T, Graces JM, Jerome R. Polyethylene-Layered Silicate Nanocomposites Prepared by The Polymerization-Filling Technique: Synthesis and Mechanical Properties. Polymer 2002; 43(8): 2123. https://doi.org/10.1016/S0032-3861(02)00036-8

[49] Ren J, Huang Y, Liu Y, Tang X. Preparation, Characterization and Properties of Poly(Vinyl Chloride)/Compatibilizer/Organophilic-Montmorillonite Nanocomposites by Melt Intercalation. Polymer Testing 2005; 24(3): 316. https://doi.org/10.1016/j.polymertesting.2004.11.004

[50] Wang MS, Pinnavaia TJ. Clay-Polymer Nanocomposites Formed from Acidic Derivatives of Montmorillonite and An Epoxy Resin. Chemistry Materials 1994; 6(4): 468. https://doi.org/10.1021/cm00040a022

[51] Lan T, Pinnavaia TJ. Clay-Reinforced Epoxy Nanocomposites. Chemistry Materials 1994; 6(12): 2216. https://doi.org/10.1021/cm00048a006

[52] Kelly P, Akelah A, Qutubuddin S, Moet A. Reduction of Residual Stress in Montmorillonite/Epoxy Compounds. Journal of Materials Science 1994; 29(9): 2274. https://doi.org/10.1007/BF00363414

[53] Önal M, Çelik M. Polymethacrylamide/Na-Montmorillonite Nanocomposites Synthesized by Free-Radical Polymerization. Materials Letters 2006; 60(1): 48. https://doi.org/10.1016/j.matlet.2005.07.069

[54] Çelik M. Graft Copolymerization of Methacrylamide onto Acrylic Fibers Initiated by Benzoyl Peroxide. Journal of Applied Polymer Science 2004; 94(4): 1519. https://doi.org/10.1002/app.21073

[55] Azab MM. Study of The Copolymerization Parameters of 2-Thiozyl Methacrylamide With Different Alkyl Acrylates. Journal of Polymer Research 2005; 12(1): 9. https://doi.org/10.1007/s10965-004-0655-y

[56] Önal M, Sarıkaya Y, Alemdaroğlu T, Bozdoğan İ. Isolation and Characterization of A Smectite As A micro-Mesoporous Material From A Bentonite. Turkish Journal of Chemistry 2003; 27(6): 683. IDS Number: 762DM

[57] Li Y, Zhao B, Xie S, Zhang S. Synthesis and Properties of Poly(Methyl Methacrylate)/Montmorillonite (PMMA/MMT) Nanocomposites. Polymer International 2003; 52(6): 892. https://doi.org/10.1002/pi.1121

[58] Zhang W, Li Y, Wei L, Fang Y. In situ Intercalative Polymerization of Poly(Methyl Methacrylate)/Clay Nanocomposites by γ-Ray Irradiation. Materials Letters 2003; 57(22-23): 3366. https://doi.org/10.1016/S0167-577X(03)00076-4

[59] Fu X, Qutubuddin S. Polymer–Clay Nanocomposites: Exfoliation of Organophilic Montmorillonite Nanolayers in Polystyrene. Polymer 2001; 42(2): 807. https://doi.org/10.1016/S0032-3861(00)00385-2

[60] Ratna D, Manoj NR, Varley R, Singh Raman RK, Simon GP. Clay-Reinforced Epoxy Nanocomposites. Polymer International 2003; 52(9): 1403. https://doi.org/10.1002/pi.1166

[61] Chen Z, Huang C, Liu S, Zhang Y, Gong K. Synthesis, Characterization and Properties of Clay-Polyacrylate Hybrid Materials. Journal of Applied Polymer Science 2000; 75(6): 796. https://doi.org/10.1002/(SICI)1097-4628(20000207)75:6<796::AID-APP8>3.0.CO;2-#

[62] Altın O, Özbelge HÖ, Doğu T. Effect of pH in An Aqueous Medium on The Surface Area, Pore Size Distribution, Density, And Porosity of Montmorillonite. Journal of Colloid Interface Science 1999; 217(1): 19. https://doi.org/10.1006/jcis.1999.6271

[63] Gregg SJ, Sing KSW. Adsorption, Surface Area and Porosity. Academic Press, London. 1982. https://doi.org/10.1002/bbpc.19820861019

[64] Khalil T, Abou El-Nour F, El-Gammal B, Boccaccini AR. Determination of Surface Area and Porosity of Sol–Gel Derived Ceramic Powders in The System TiO2–SiO2–Al2O3 Powder Technology 2001; 114(1-3): 106. https://doi.org/10.1016/S0032-5910(00)00271-0

[65] Passe-Coutrin N, Altenor S, Cossement D, Jean-Marius C, Gaspard S. Comparison of Parameters Calculated From The BET and Freundlich Isotherms Obtained by Nitrogen Adsorption on Activated Carbons: A New Method for Calculating The Specific Surface Area. Microporous and Mesoporous Materials 2008; 111(1-3): 517. https://doi.org/10.1016/j.micromeso.2007.08.032

[66] Shujun C, Rongshun W. Surface Area, Pore Size Distribution and Microstructure of Vacuum Getter. Vacuum 2011; 85(10): 909. https://doi.org/10.1016/j.vacuum.2010.11.012

[67] Downie A, Crosky A, Munroe P. Physical Properties of Biochar, Biochar for Environment Managemen Science and Technology. Earthscan p.13-32, London. 2009.

Received on 13-09-2019 Accepted on 04-10-2019 Published on 18-10-2019

DOI: https://doi.org/10.31875/2410-4701.2019.06.4